

Shadow Effects in Spiral Phase Contrast Microscopy

Alexander Jesacher, Severin Fürhapter, Stefan Bernet, and Monika Ritsch-Marte

Division of Biomedical Physics, Medical University of Innsbruck, Müllerstr. 44, A-6020 Innsbruck, Austria
(Received 17 December 2004; revised manuscript received 15 March 2005; published 15 June 2005)

Recently it has been demonstrated that spatial filtering of images in microscopy with a spiral phase element in a Fourier plane of the optical path results in a strong edge enhancement of object structures. In principle the operation is isotropic, i.e., all phase edges of a sample object are highlighted simultaneously, independent of their local direction. However, here we demonstrate that the symmetry can be broken intentionally by controlling the phase of the central area of a spiral phase hologram, which is displayed at a computer controlled spatial light modulator. This produces an apparent shadow effect which can be rotated at video rate. The resulting relieflike impression of the sample topography with a longitudinal resolution in the subwavelength regime is demonstrated by imaging a standard low contrast test sample consisting of a human cheek cell.

DOI: 10.1103/PhysRevLett.94.233902

PACS numbers: 42.30.Kq, 42.30.Va, 42.40.Eq

In a few recent articles, it has been suggested that coherent spatial image filtering with a spiral phase element leads to a strong edge contrast enhancement of both amplitude [1–3] and phase objects [4]. The method is related to other spatial filtering operations used in microscopy: Dark-field and Dodt microscopy [5] use Fourier filters which are partially absorptive, and thus lose some image intensity. Phase contrast microscopy shifts the phase of the zero-order Fourier component of the object wave, imaging a phase sample as an intensity modulated picture. In contrast, spiral phase filtering is not sensitive to the absolute phase of a sample, but to phase gradients, which are strongly amplified by redistribution of the image intensity. This is similar to the established Nomarski (or differential interference contrast) method, however without the need to manipulate the polarization of the image wave. Spiral phase filtering differs from earlier reported fractional Hilbert transform filtering [6] by the rotational symmetry of the phase filter mask, resulting in an isotropic filter effect, i.e., all edges of a sample object are highlighted simultaneously, independent of their local direction.

However, here we will demonstrate that for some applications it can be advantageous to break the circular symmetry of the “ideal” spiral phase operation, creating an oriented shadow effect. This is done by manipulating the phase of the zero-order Fourier component of the image wave in another way than the remaining light. The direction of the shadow can be continuously controlled through the phase of the central area, and it differs by 90° when imaging objects with phase- or amplitude contrast. This results in strongly edge-enhanced relieflike views of microscopic samples, which allow us to identify the sample topography with subwavelength axial resolution.

Consider a spiral phase element that applies an angular-dependent phase shift of the form $\exp(i\varphi)$ to the wave front of an incoming light wave, either by transmission through (or reflection from) a correspondingly shaped refractive index plate, or in our case, by diffraction from a corresponding hologram [7]. There, φ is the polar angle mea-

sured from the center of the spiral phase element. Such spiral phase elements are, for example, used to create Laguerre-Gaussian beams (“doughnut beams”) from an incoming Gaussian light wave. Such a spiral phase element has a singularity in its center, i.e., there the phase is not defined. However, the singularity is usually not important for practical purposes. For example, it does not influence the creation of a doughnut beam from an incoming Gaussian (or “plane”) wave, since only a negligible fraction of the total light intensity is located at the central point.

The situation is changed, however, if such a spiral phase element is used as a spatial filter for Fourier plane filtering of an incoming, image carrying light wave. The reason is that the zero-order Fourier spot of the incoming light field (also denoted as the carrier wave) contains most of the total intensity of the image wave and focuses at the central point of the spiral phase element. Obviously, it now makes a strong difference for the reassembled light field in the image plane, whether this central spot is absorptive, or whether it acts as a phase shifter.

A numerical simulation illustrating these effects is sketched in Fig. 1. Image 1(a) visualizes a simulated complex sample surface, consisting of refractive and absorptive

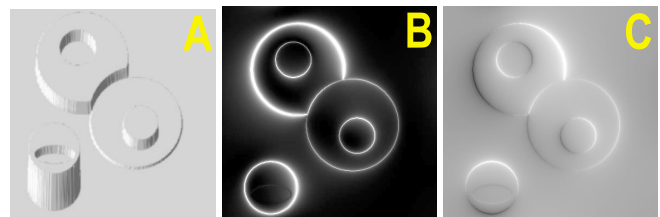


FIG. 1 (color online). Simulation of a combination of amplitude and phase objects imaged by a spiral phase contrast filter. (a) shows the “sample object” to be imaged as a relief. (b) shows the numerically computed result for spatial filtering of the image wave with an ideal spiral phase element with a singular center point which is absorptive. (c) shows the result after filtering with a spiral phase element with a transmissive center, resulting in a relieflike view of the sample.

regions, by displaying the real part of the transmission function as a relief. The two intersecting spheres in the upper part are simulated phase objects, whereas the structure in the lower left corner is an amplitude object. The phase contrast between the right sphere and its background is set to $0.04 \times 2\pi$, corresponding to an optical path length difference of 4% of a wavelength. The amplitude contrast between the sphere in the lower left edge, and the elliptic pit in its surface is set to 20%. Image 1(b) shows the result of a numerically performed spatial filtering operation of the image wave with a “perfect” spiral phase element with a single absorptive pixel in its center. The computation was performed by applying a fast Fourier transform to the complex image field, then multiplying pixel by pixel with a complex spiral transmission function of the form $\exp(i\varphi)$, followed by a reverse Fourier transform to the image plane, where the image intensity (squared absolute value) is displayed. The same sequence of operations is performed by the optical elements in our experiment by a first Fourier transforming lens for the image wave, then a spiral phase mask in its Fourier plane, and a back-transforming lens at a focal distance. As a result, the filtered image 1(b) shows a strong and isotropic edge amplification, displaying, for example, longitudinal phase jumps in the far subwavelength regime [4].

Image 1(c) shows the result of an analogous spatial filtering operation, however now with a transmissive central pixel of the spiral phase element. The image clearly displays the topography of the sample, e.g., troughs and ridges in the phase structures are distinguished by an apparent shadow effect. Furthermore, there is a 90° difference in the orientation of the shadow between the phase structures (upper intersecting spheres) and the amplitude structure in the lower left corner, which seem to be “illuminated” from the right side and from above, respectively. This allows us to distinguish between objects with amplitude and phase contrast.

The effects can be understood by examining an ideal two-dimensional spiral phase filter in a polar coordinate system (with radial and angular coordinates of r and φ , respectively), and considering it as composed of an infinite number of radially proceeding one-dimensional Fourier filters at continuously changing polar angles, i.e., each single Fourier filter consists of a straight line passing through the center of the spiral phase plate. Each of these one-dimensional filters controls the appearance of the two-dimensional image structures in a direction perpendicular to its course. Regarding one individual “filter ray” with the direction φ , the corresponding transmission function $T(x)$ consists of a signum function [defined as $\text{sgn}(x) = 1$ for $x > 1$, $\text{sgn}(x) = -1$ for $x < 1$, and $\text{sgn}(x) = 0$ for $x = 0$], multiplied by a phase factor corresponding to the polar angle φ , i.e., $T(x) = \text{sgn}(x) \exp(i\varphi)$. There, x is the coordinate along a diagonal line in the direction φ , with $x = 0$ denoting the center of the spiral phase plate. Note that $T(0) = 0$, i.e., the central point at $x = 0$ has zero transmission. Using such a function as a one-dimensional spa-

tial filter produces the so-called Hilbert transform of the original function [2,6,8].

The one-dimensional Hilbert transform of a function looks similar to its derivative, i.e., it strongly amplifies sharp gradients (or steps) of the original function. Furthermore, the Hilbert transform changes the symmetry of a function, i.e., the amplitudes of up- and down-directed steps get a different sign. However, the absolute values of these amplitudes are still the same, such that up- and down-directed steps are not distinguished in imaging applications. Generalized to the two-dimensional case, this situation applies to the isotropic edge contrast enhancement of ideal spiral phase filtering [2,4].

Nevertheless, it is possible to reveal the sign of the field amplitude in the intensity distribution of the filtered function by superposing it interferometrically with a plane wave. Such a plane wave is “automatically” generated from the zero-order Fourier spot of the original image wave, if it is not absorbed in the center of the filter mask, but just phase shifted by an adjustable phase offset θ . This single central spot in the Fourier plane evolves to a plane wave in the image plane, which interferes with the complex amplitude distribution generated by the Hilbert transform. The resulting superposition is determined by the interference term $\exp[i(\varphi - \theta)]$ and leads to a continuously adjustable amplification or attenuation of positive or negative field amplitudes which correspond to the edges of troughs and ridges within the sample.

Returning to the two-dimensional spiral transform, the asymmetry of the shadow effect results from the fact that the interference term $\exp[i(\varphi - \theta)]$, which determines the direction in which the edge amplification effect is maximally asymmetric, depends on φ itself. Such an edge contrast, which is a function of the polar direction φ , creates the impression of a shadow at a structured surface which is illuminated from an oblique direction.

The same reasoning also predicts the appearance of a $\pi/2$ -phase shift in the shadow directions of amplitude and phase samples. This is due to the fact that the difference between image waves with amplitude and phase contrast also consists in a $\pi/2$ relative phase offset between their respective zero-order Fourier components and their higher order Fourier terms [9]. This $\pi/2$ offset contributes to their respective θ values within the interference term $\exp[i(\varphi - \theta)]$, and results in a corresponding $\pi/2$ difference in their respective shadow orientations.

Our experimental setup is sketched in Fig. 2. The sample object to be imaged is placed in the object plane of a standard inverted microscope (Zeiss Axiovert 135) and is illuminated in transmission geometry from above with a collimated white light beam emerging from a fiber (diameter $D_f = 400 \mu\text{m}$). A microscope objective (magnification 60x, numerical aperture $\text{NA} = 1.25$) is used for imaging. Spatial filtering of the imaging light wave is done in a Fourier plane of the setup. A relay system consisting of a set of two lenses images the rear Fourier

plane of the microscope objective to another plane outside of the microscope. The exact position of the Fourier plane is determined by the focus of the illumination light. There, a reflective spatial light modulator (Holoeye 3000 system, resolution 1920×1200 square pixels with a pixel size of $10 \mu\text{m}$ [10]) is placed, which can display blazed phase holograms. For ideal spiral phase filtering, a hologram is displayed which has a forklike helical discontinuity in its center [see image (a)], which coincides with the focused zero-order Fourier spot of the imaging light wave. The incident light wave is diffracted with an absolute diffraction efficiency of approximately 30%, and only the light in the first diffraction order is used for further imaging, after blocking undesired other diffraction orders with a diaphragm (not indicated in the figure). Imaging is then performed with a third lens located symmetrically (at a focal distance) between the spatial light modulator (SLM) and a CCD camera.

In order to produce the modified spiral phase filter which generates the desired shadow effect, the central part of the hologram [1(a)] is substituted by a circular area which just acts as a blazed grating, diffracting the incident light into the same direction as the spiral phase hologram [see Fig. 2(b), not to scale]. The phase of the inner blazed grating controls the phase of the diffracted zero-order Fourier component of the incident light field, and thus the interference angle θ mentioned before. A continuous phase shift of this inner grating in a range between 0 and 2π results in a rotation of the apparent shadow direction by 360° . In the numerical simulations the zero-order Fourier component of the image wave is defined by one single pixel in the center of the calculated pixel array, and therefore its relative “area” with respect to the remaining image depends on the digital image resolution. For practical purposes however, the diameter D of the zero-order Fourier component in the SLM plane corresponds to the diameter of the sharply imaged illumination fiber output. Thus, D is given by the optical parameters of the setup: $D = D_f m f_{\text{obj}} / f_c$, where $f_c = 80 \text{ mm}$ is the focal length

of the fiber collimation lens, $f_{\text{obj}} = 19 \text{ mm}$ is the rear focal length of the microscope objective, and $m = 2$ is a magnification factor introduced by the relay-lens system. In our case we obtain $D \approx 190 \mu\text{m}$. Practically, the optimal diameter of the inner grating is found by experimentally adjusting it for a maximal shadow contrast.

The holograms are computed by first calculating the phase profile of a standard spiral phase plate ($\sim \exp(i\varphi)$), then attaching a certain phase value θ to a small circular area $A(x, y)$ in the center of the phase mask [i.e., $A(x, y) = \exp(i\theta)$], and finally multiplying with an inclined plane phase term of the form $\exp(iG_x x + iG_y y)$ in order to produce a blazed off-axis hologram diffracting into a direction \vec{G} . The phase angle of the result of the above operations is computed (modulo 2π) and displayed as a phase hologram at the SLM, i.e., gray levels are converted to phase offsets by the display.

An example is shown in Fig. 3. The figure displays a sequence of five images taken from a test sample with a very low phase contrast, i.e., a human cheek cell. Figure 3(a) shows a bright-field image of the sample obtained by using the SLM as a simple blazed grating. Obviously, the cheek cell cannot be recognized. Figures 3(b) and 3(c) show two exposures of the cheek cell obtained by filtering with a symmetry-breaking spiral phase hologram [Fig. 2(b)]. The difference between 3(b) and 3(c) is that the phase of the central grating is shifted by π , resulting in two images where the apparent shadow directions seem to be opposed. The filtered images resemble a relieflike surface structure, which is illuminated from an oblique direction. The two images reveal details of the cheek cell, like its core (central elliptic structure) and small bacteria at the cell membrane. In the experiment it was possible to rotate the shadow direction by continuously changing the displayed hologram. This gives the impression of a sample that is illuminated by a circling spotlight, which is useful for clearly identifying the whole silhouette of the imaged object. Furthermore, this suggests

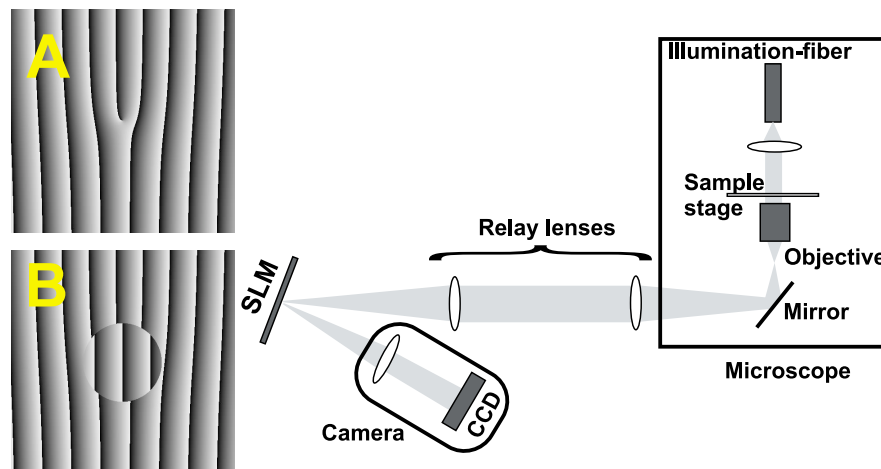


FIG. 2 (color online). Sketch of our experimental setup. Details are explained in the text.

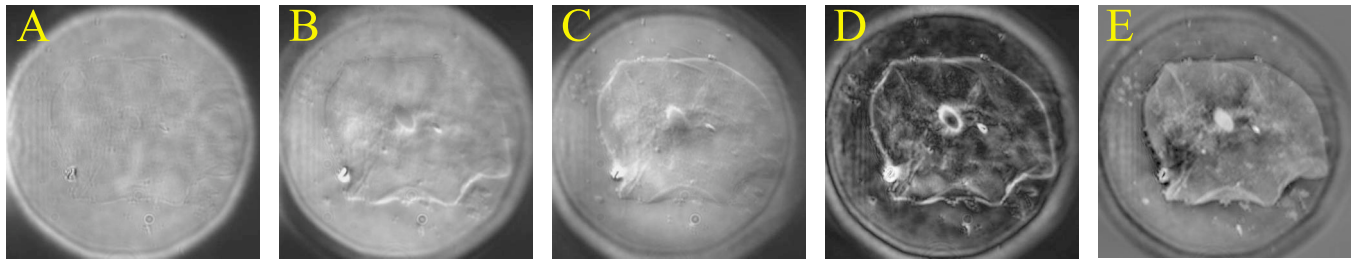


FIG. 3 (color online). Imaging of a human cheek cell. The image diameter is $\sim 50 \mu\text{m}$. (a) Bright-field image. (b) Resulting image after spatial filtering of the original image wave with the symmetry-breaking spiral phase hologram shown in Fig. 2(b). (c) Same spiral-filtering method as in (b), however, the phase of the central blazed grating is offset by π . (d) Absolute value of the complex image composed of 12 shadow effect images recorded with a phase offset of $2\pi/12$ from exposure to exposure. (e) Two-dimensional Hilbert back transform applied to image (d), looking similar as phase contrast microscopy, however with enhanced resolution.

a subsequent digital image processing step: Fig. 3(d) shows the absolute value of a complex image, obtained by summing 12 individual shadow effect images with continuously changing shadow directions in a range between 0 and 2π , i.e., recorded with a phase offset of the central grating of 30° from exposure to exposure. Each individual image n was then multiplied with its corresponding complex phase factor $\exp(i2\pi n/12)$ before the summation over all images was performed. The operation results in an image with an apparently isotropic edge amplification, removing any unmodulated structures in the image which are not influenced by the interference phase term. However, the phase-angle data of the resulting complex image still includes the orientational information contained in the individual shadow effect images. This makes it possible to further process the complex image [3(d)] by applying a reverse two-dimensional Hilbert transform, i.e., a convolution of the image data with $\exp[-i\varphi(x, y)]$. The absolute value of the result of this operation is plotted in Fig. 3(e). It shows an image of the test sample which displays the different phase levels with intensity contrast, similar to phase contrast microscopy, however with a strongly enhanced phase resolution, and an efficient background suppression due to the coherent averaging operation. Compared to a Nomarski system, the method is expected to have a superior resolution, and the advantage that the gradient contrast direction can be changed continuously without any mechanical manipulation, and without the requirement of polarization control.

The modification of spiral phase contrast microscopy by combining it with a symmetry-breaking central phase shifter for the zero-order Fourier component has a significant potential in optical microscopy. It produces a relieflike view of the sample topography with a longitudinal sub-wavelength resolution and can be easily implemented into the optical path of standard microscopes. In principle the method can be performed with a static spiral phase element like a wave plate or a static hologram, however, combining it with an electronically controllable SLM offers the additional possibility of rotating the shadow without any mechanically moving components. Interestingly the method

emanates from a recently introduced generalization of the one-dimensional Hilbert transform to two dimensions, which was first suggested as a mathematical operation in digital imaging processing applications [11–13], but which is here directly implemented as an optical method. Because of the sensitivity of the Hilbert operation to phase gradients, this kind of microscopy is optimal for the detection of crystal dislocations (e.g., in semiconductors), or for microscopic imaging of biological samples with a low phase contrast.

The authors want to acknowledge funding by the Austrian Science Foundation (FWF), Project No. P18051-N02, and by the Austrian Academy of Sciences (A. J.).

-
- [1] K. Crabtree, J. A. Davis, and I. Moreno, *Appl. Opt.* **43**, 1360 (2004).
 - [2] J. A. Davis, D. E. McNamara, D. M. Cottrell, and J. Campos, *Opt. Lett.* **25**, 99 (2000).
 - [3] G. A. Swartzlander, Jr., *Opt. Lett.* **26**, 497 (2001).
 - [4] S. FÜRhapter, A. Jesacher, S. Bernet, and M. Ritsch-Marte, *Opt. Express* **13**, 689 (2005).
 - [5] A sketch of a Dodt-setup can be found, e.g., in R. Yasuda *et al.*, *STKE* **219**, 15 (2004).
 - [6] A. W. Lohmann, E. Tepichin, and J. G. Ramirez, *Appl. Opt.* **36**, 6620 (1997).
 - [7] J. Arlt, K. Dholakia, L. Allen, and M. J. Padgett, *J. Mod. Opt.* **45**, 1231 (1998).
 - [8] *The Fourier Transform and its Applications*, edited by R. Bracewell (McGraw-Hill, New York, 1965).
 - [9] *Physical Optics Notebook: Tutorials in Fourier Optics*, edited by G. O. Reynolds, J. B. DeVelis, G. B. Parrent, Jr., and B. J. Thompson (SPIE Optical Engineering Press, Bellingham, Washington, 1989).
 - [10] A. Jesacher, S. FÜRhapter, S. Bernet, and M. Ritsch-Marte, *Opt. Express* **12**, 2243 (2004).
 - [11] M. R. Arnison, K. G. Larkin, C. J. R. Sheppard, N. I. Smith, and C. J. Cogswell, *J. Microsc.* **214**, 7 (2004).
 - [12] M. R. Arnison, C. J. Cogswell, N. I. Smith, P. W. Fekete, and K. G. Larkin, *J. Microsc.* **199**, 79 (2000).
 - [13] K. G. Larkin, D. J. Bone, and M. A. Oldfield, *J. Opt. Soc. Am. A* **18**, 1862 (2001).